Supporting Information: Distinguishing the Mechanism of Electrochemical Carboxylation in CO$_2$ eXpanded Electrolytes

Matthew A. Stalcup[1,3], Christian K. Nilles[2,3], Bala Subramaniam[*1,3,a], James D. Blakemore[*2,3,b], and Kevin C. Leonard[*1,3,c]

[1]Department of Chemical & Petroleum Engineering, The University of Kansas, Lawrence, KS USA
[2]Department of Chemistry, The University of Kansas, Lawrence, KS USA
[3]Center for Environmentally Beneficial Catalysis, The University of Kansas, Lawrence, KS USA

[a]bsubramaniam@ku.edu
[b]blakemore@ku.edu
[c]kcleonard@ku.edu

Contents

List of Figures

List of Tables

1 Detailed Description of Experimental Methods and Equipment

1.1 Electrochemical Methods

High-pressure electrochemical experiments were performed in a single-cell electrochemical vessel as described elsewhere.[1,2] Briefly, this vessel was custom-built from a Parr reactor fitted with a modified cap and electrical feed-throughs capable of withstanding the operating pressure of the reactor. Inside the reaction vessel, a glass cylinder separated the electrochemical solution, consisting of 0.4 M tetrabutylammonium hexafluorophosphate in acetonitrile, from the metal body of the reactor. The reactor was fitted with temperature and pressure sensing equipment that is monitored with a National Instruments LabVIEW®Data Acquisition system. The reactor is jacketed by a custom-built single pass heat exchanger piped to a water bath allowing for precise temperature control ensuring isothermal reaction conditions.

All electrochemical experiments were performed with a Gamry Reference 3000 Potentiostat/ Galvanostat at various CO_2 pressures (Matheson 99.999% purity) and a constant temperature of 25 °C using a glassy carbon working electrode (0.0079 cm^2), a sacrificial magnesium counter electrode (99.9% purity), and a silver wire inside a fritted chamber quasi-reference (99.9% purity). The reaction medium consisted of acetonitrile, 0.4 M tetrabutylammonium hexafluorophosphate (TBAPF$_6$), 4 mM ferrocene (Fc), and 100 mM acetophenone. All components of the solution were thoroughly dried to remove trace water impurities.

Previous work has shown that the ferrocene redox couple can be used as an internal reference over the pressure and potential ranges studied.[1] The potential of the Ag quasi-reference electrode was calibrated against the potential of the Fc$^{+/0}$ redox couple for each electrochemical experiment.

The Mg sacrificial anode was used to enable the study of the electrochemical carboxylation reduction reactions without drastically changing the reaction media. Without the use of a sacrificial anode, the supporting electrolyte and/or solvent may be oxidized on a more conventional platinum counter electrode, which disrupts the system and produces unwanted side products.[3]

1.2 COMSOL Multiphysics Simulation of Voltammetry

COMSOL (COMSOL Multiphysics® v. 6.0) simulations were used to model the physicochemical processes underlying electrochemical carboxylation of acetophenone on a glassy carbon electrode in CO_2 expanded electrolytes. The simulation field is shown in Fig. S1. The simulated reactor geometry was created as a 2D axial-symmetric domain with the electrode size (0.5 mm radius), insulating sheath size (100 μm width), and reactor dimensions (5 mm radius, 8 mm height). This reactor size was chosen because it is sufficiently larger than the boundary layer surrounding the electrode. Thus, the CO_2 and the acetophenone concentration at the outer boundary is the same as the well-mixed reactor bulk concentration. A free triangular mesh using COMSOL's built-in 'normal' element size was used for the bulk of the reactor, with a 'fine' mesh used for the area near the electrode (1 mm × 1 mm). An edge mesh was incorporated with a maximum mesh element of 1×10^{-4} mm and a minimum mesh element of 1×10^{-4} mm for increased spatial resolution near the electrode. The transport of the reactants to and from the electrode surface was simulated by the "transport of diluted species" module in COMSOL. This module evaluates Fick's Second Law of diffusion, eq. (S1), to model the concentration gradients and the development of the diffusion layer near the electrode.

$$\frac{\partial C_i}{\partial t} = D_i \nabla^2 C_i \tag{S1}$$

Previous studies have provided us with accurate measurements of the CO_2 concentration as a function of the headspace pressure.[1] These experimentally determined values were used as initial

conditions for the bulk concentration of the CO_2 species in the simulated system.

In addition, our previous studies found that the diffusion coefficient in CXE media increases with CO_2 pressure.[1] In this study, we found that a regressed diffusion coefficient for acetophenone of 2.5×10^{-5} $cm^2\,s^{-1}$ best fit the experimental cyclic voltammetry data under Ar-saturated conditions. Under CXE conditions, we found that the model predicted an increase in the diffusion coefficient to 3.2×10^{-5} $cm^2\,s^{-1}$, consistent with our earlier report.[1]

The acetophenone concentration was also fixed at 100 mM at each CO_2 pressure. Experimentally, this was achieved by adjusting the volume of acetophenone initially added to the reactor based on knowledge of the increase in CXE volume as a function of CO_2 pressure.[1] Additionally, "No Flux" boundary conditions were placed at the boundaries of the reactor geometry to define the areas where a mass transfer can occur. A "Flux" boundary condition was placed at the surface of the electrode to allow the flow of electrons to the substrate.

Butler-Volmer kinetics were then used to model the electrochemical behavior as a function of electrode potential. The Butler-Volmer kinetic model, eq. (S2), calculates the change in the reaction rate as the electrode potential changes. Elementary reaction kinetics were used to represent the addition of CO_2 to the acetophenone radical. The partial current density for each electron transfer step was used to calculate the total current. Constants for this equation fundamentally influence the shape of the voltammetry. This equation also contains the fundamental kinetic information that can be used to model this system accurately. The electrochemical rate constants(k_1^0, k_3^0) in addition to the standard reduction potentials (E_0^1, E_0^3) are adjusted to make the model fit the experimental data. Once these parameters are inputted into the system, the current flowing from the electrode is determined by the potential and the concentration of the redox species.

$$i = FAk^0 \left[C_O(0,t)e^{-\alpha f(E-E^{0\prime})} - C_R(0,t)e^{(1-\alpha)f(E-E^{0\prime})} \right] \tag{S2}$$

Aside from electrochemical kinetics, homogeneous chemical kinetics must also be simulated to model the intermediate chemical reaction step between the electron transfer reactions. The rate of this chemical reaction step depends on the concentration of acetophenone, the reaction rate constant k_2, and most importantly the concentration of liquid phase CO_2. Each of these parameters is required to fit the pressure-dependent effects of CO_2 concentration in the liquid phase on the electrochemical carboxylation of acetophenone. Initial estimates for the electrochemical and chemical rate constants as well as the standard reduction potentials for eq. (S2) were used to begin the simulation of the system.

Specifically, the boundary equations for the FEA are as follows. Along any non-reactive edge, including all of the reactor walls and the insulating sheath of the electrode, we used a no-flux boundary condition in the transport of diluted species module. The electrolyte plane was set to axial symmetry for the 2D-axial symmetric simulation. The electrode had a flux boundary condition, where the flux of each of the acetophenone species was governed by their appropriate reactions.

For example, in our ECE mechanism, there are four species–acetophenone (A), the acetophenone radical ($A^{\cdot-}$), the acetophenone-CO_2 adduct ($AC^{\cdot-}$), and the unprotonated atrolactic acid (AA^{2-}).

Using this notation, we can write reactions for each step in our ECE reaction, assuming that the electrochemical steps occur reversibly and the homogenous steps occur irreversibly.

$$r_{1,f} = k_1^0 e^{-\alpha f(E-E_1^{0\prime})}[A] \tag{S3a}$$

$$r_{1,b} = k_1^0 e^{(1-\alpha)f(E-E_1^{0\prime})}[A^{\cdot-}] \tag{S3b}$$

$$r_2 = k_2[CO_2][A^{\cdot-}] \tag{S3c}$$

$$r_{3,f} = k_3^0 e^{-\alpha f(E-E_3^{0'})}[AC^{\cdot-}] \tag{S3d}$$

$$r_{3,b} = k_3^0 e^{(1-\alpha)f(E-E_3^{0'})}[AA^{2-}] \tag{S3e}$$

At the surface of the electrode, the flux of each species is then given by:

$$J_A = -r_{1,f} + r_{1,b} \tag{S4a}$$

$$J_{A^{\cdot-}} = r_{1,f} - r_{1,b} \tag{S4b}$$

$$J_{AC^{\cdot-}} = -r_{3,f} + r_{c,b} \tag{S4c}$$

$$J_{AA^{2-}} = r_{3,f} - r_{c,b} \tag{S4d}$$

A reaction was then set for the electrolyte domain to model the homogeneous reaction steps as follows:

$$R_{A^{\cdot-}} = -r_2 \tag{S5a}$$

$$R_{CO_2^-} = -r_2 \tag{S5b}$$

$$R_{AC^{\cdot-}} = r_2 \tag{S5c}$$

Finally, once the model solves for all of the rates and fluxes, the total current can be calculated by integrating the fluxes over the surface of the electrode.

$$i = F \int_0^{2\pi} \int_0^a (r_{1,f} - r_{1,b} + r_{3,f} - r_{3,b}) \, r' dr' d\theta \tag{S6}$$

where a is the radius of the electrode.

Manual optimization of each parameter was initially carried out at one pressure and scan rate. Once the fit was acceptable further optimization was done using different scan rates (50, 100, 200, and 500 mVs^{-1}) at 28.6 bar to validate the fit to the experimental data. Further testing of the model fit was carried out at various CO_2 pressures where the only changes to the model were the scan rate and the concentration of CO_2 in the liquid phase. The results of the simulations are found in table S1.

Table S1. Optimized parameters for the simulation of cyclic voltammetry experiments of the acetophenone reduction reaction.

CO_2 Pressure bar	$[CO_2]$ M	[Acetophenone] M	k_1^0 cm/s	E_1^0 V vs. Fc^+/Fc	k_2 m^3/(s mol)	k_3^0 cm/s	E_3^0 V vs. Fc^+/Fc
0	0	0.1	1.6E-3	-2.26	—	—	—
3.4, 13.8, 28.6	1.16-4.4	0.1	1.6E-3	-2.26	0.1	1.0E-3	-1.93
41.4	8.14	0.1	3.2E-4	-2.26	0.1	3.2E-5	-1.93

2 Sensitivity Analysis

To ensure that the parameters in the model were representative of the electrochemical system a sensitivity analysis was performed. The electrochemical rate constants, electrochemical potentials, and the chemical rate constant were all parameters that were optimized manually in the simulation. Each of these parameters can influence the shape of the cyclic voltammogram. The run at 13.8 bar and a scan rate of 200 mVs^{-1} were used to test the perturbations. A parametric sweep was created and iterated over different values of the parameters. The output was a simulated CV of the experimental data. This CV provided a graphical representation of the parameters that most influenced the shape of the CV. E_1^0 and k_1^0 are the parameters associated with the initial electron transfer (rate-determining) step. Changes in their value led to the greatest change in CV shape. The fit visibly worsened when the values for these parameters were either increased or decreased; however, a more concrete method of quantifying the results was desired. To quantify the accuracy of the fit, a python script was developed that would calculate the R^2 value between the simulated data and the experimental data using eq. (S7) The closer the R^2 value is to 1, the better the fit between the simulations and experimental data.

$$R^2 = 1 - \frac{\text{sum squared regression}}{\text{total sum of squares}} = 1 - \frac{\sum(y_i - \hat{y})^2}{\sum(y_i - \bar{y})^2} \tag{S7}$$

The coefficient of determination values are plotted at various parameter values to visualize the changes in the quality of the fit when the parameter value is changed. The results from the parametric sweep are found in figures Fig. S7-Fig. S11. These plots confirm that the quality of fit is most sensitive to the rate constant k_1^0 and E_1^0 of the first electrochemical reaction step in the ECE mechanism. This in turn suggests that the first electrochemical reduction step is the rate determining step.
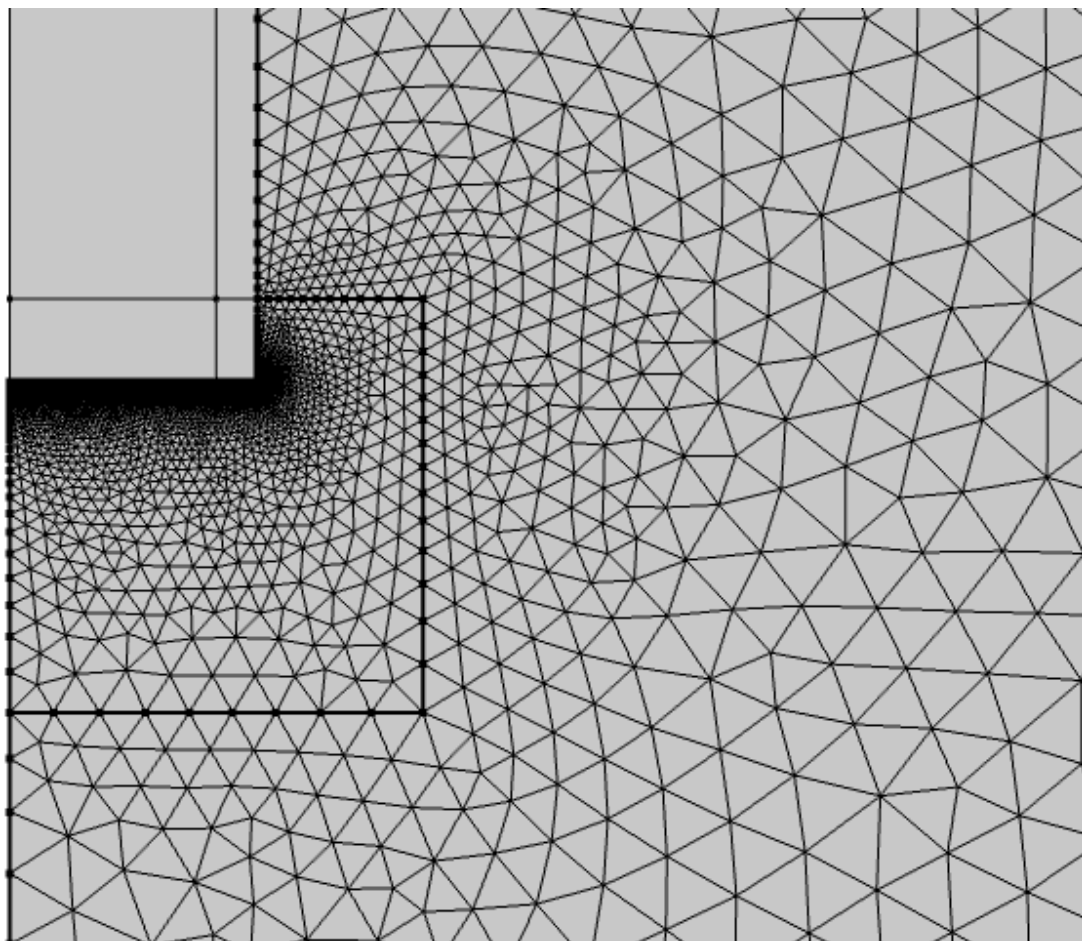
3 Supporting Information Figures

Figure S1. Simulation geometry for the COMSOL model used to represent the glassy carbon working electrode and its surrounding region.
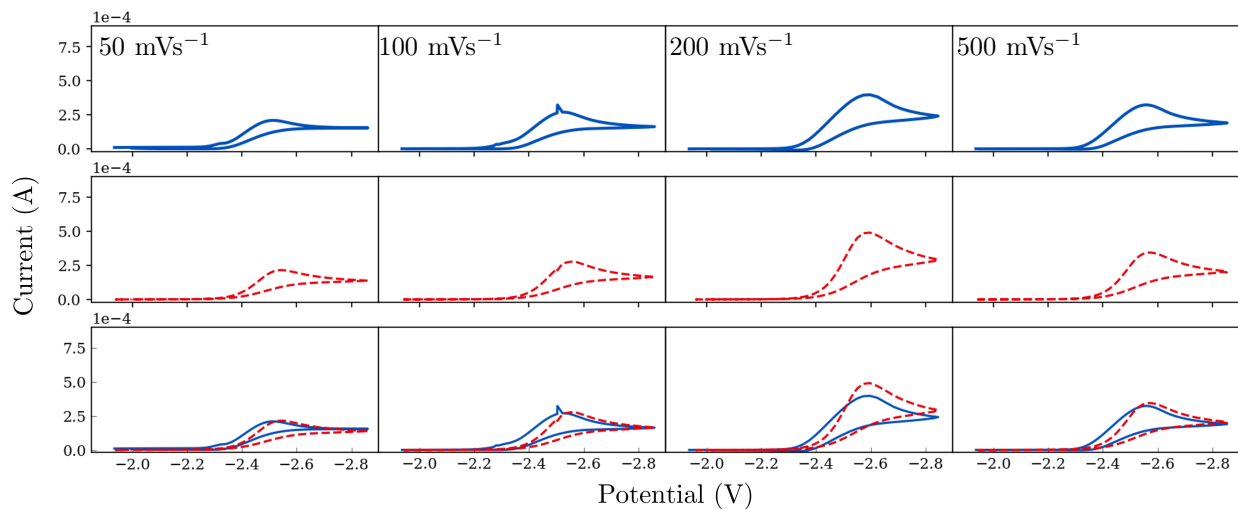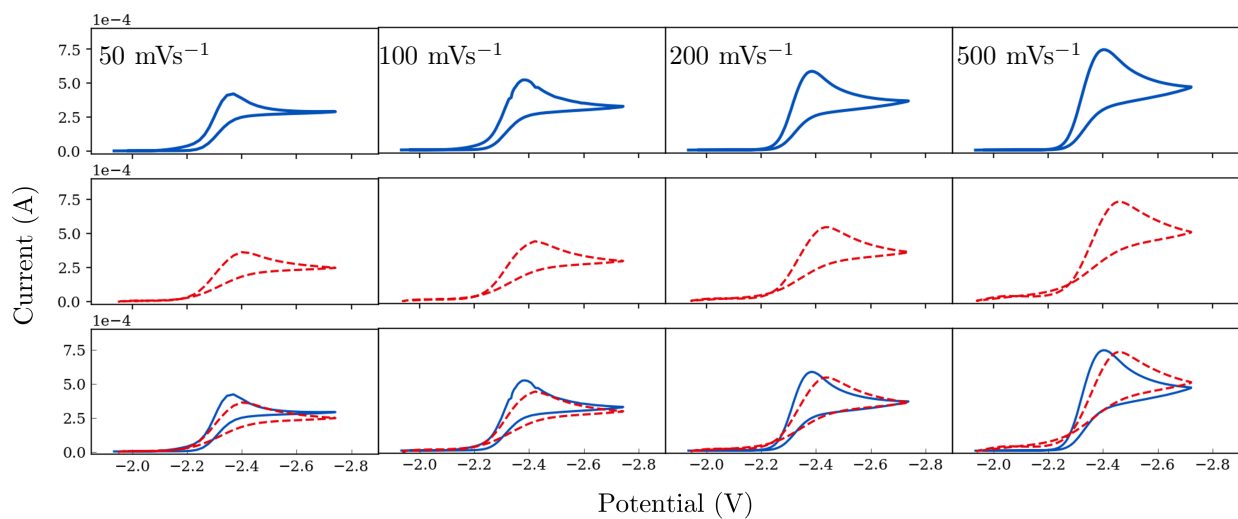
Figure S2. Comparison of cyclic voltammetry of acetophenone carboxylation at Ar saturated pressure on a 1mm diameter glassy carbon electrode (solid line) with COMSOL simulations (dashed) at various scan rates (50, 100, 200 and 500 mVs^{-1}). The bottom rows in the various panels overlay the experimental and simulated waves.
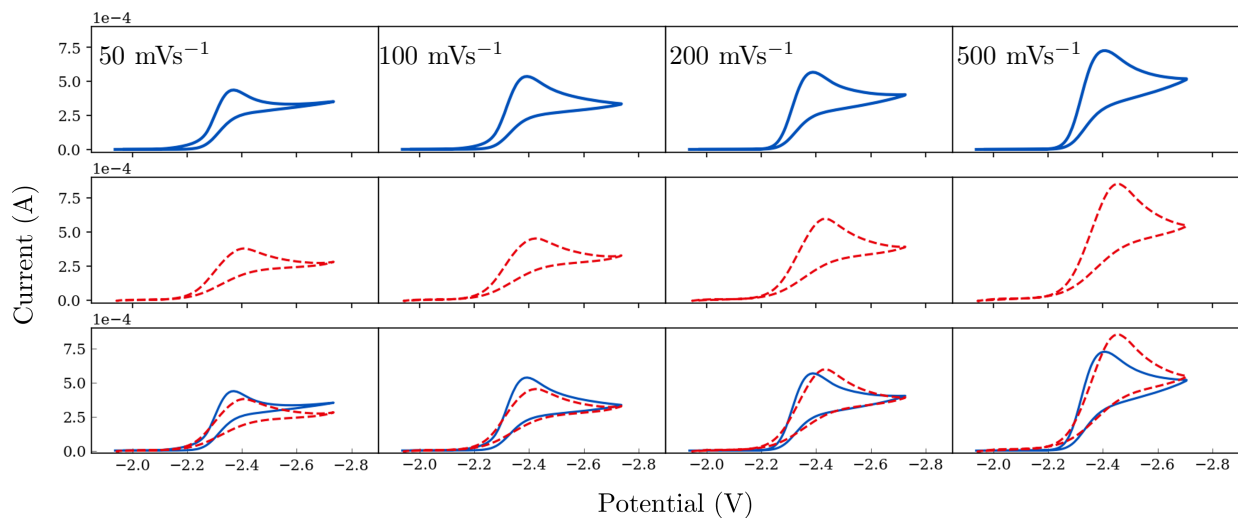

Figure S3. Comparison of cyclic voltammetry of acetophenone carboxylation at 3.4 bar CO_2 pressure on a 1 mm diameter glassy carbon electrode (solid line) with COMSOL simulations (dashed) at various scan rates (50, 100, 200 and 500 mVs^{-1}). The bottom rows in the various panels overlay the experimental and simulated waves.
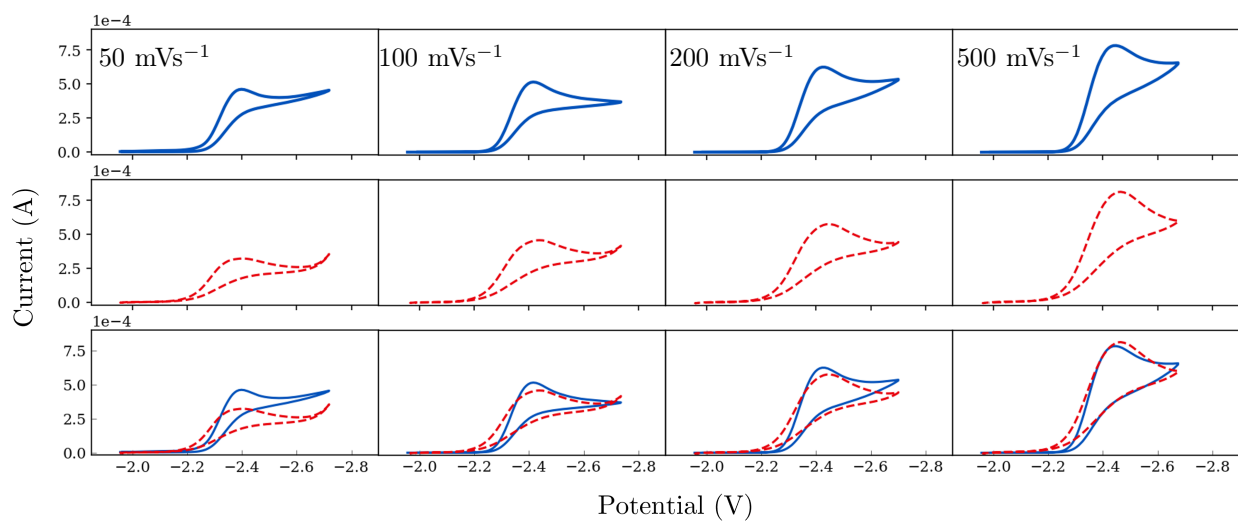
Figure S4. Comparison of cyclic voltammetry of acetophenone carboxylation at 13.8 bar CO_2 pressure on a 1 mm diameter glassy carbon electrode (solid line) with COMSOL simulations (dashed) at various scan rates ((50, 100, 200 and 500 mVs^{-1}). The bottom rows in the various panels overlay the experimental and simulated waves.
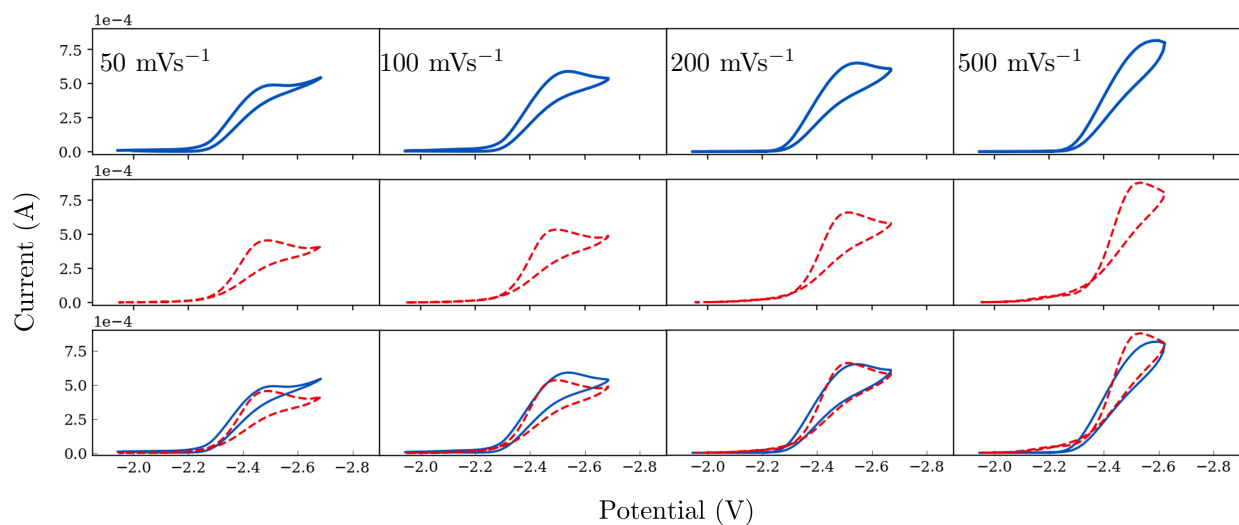

Figure S5. Comparison of cyclic voltammetry of acetophenone carboxylation at 28.8 bar CO_2 pressure on a 1 mm diameter glassy carbon electrode (solid line) with COMSOL simulations (dashed) at various scan rates (50, 100, 200 and 500 mVs^{-1}). The bottom rows in the various panels overlay the experimental and simulated waves.

Figure S6. Comparison of cyclic voltammetry of acetophenone carboxylation at 41.4 CO_2 pressure on a 1 mm diameter glassy carbon electrode (solid line) with COMSOL simulations (dashed) at various scan rates (50, 100, 200 and 500 mVs^{-1}). The bottom rows in the various panels overlay the experimental and simulated waves.
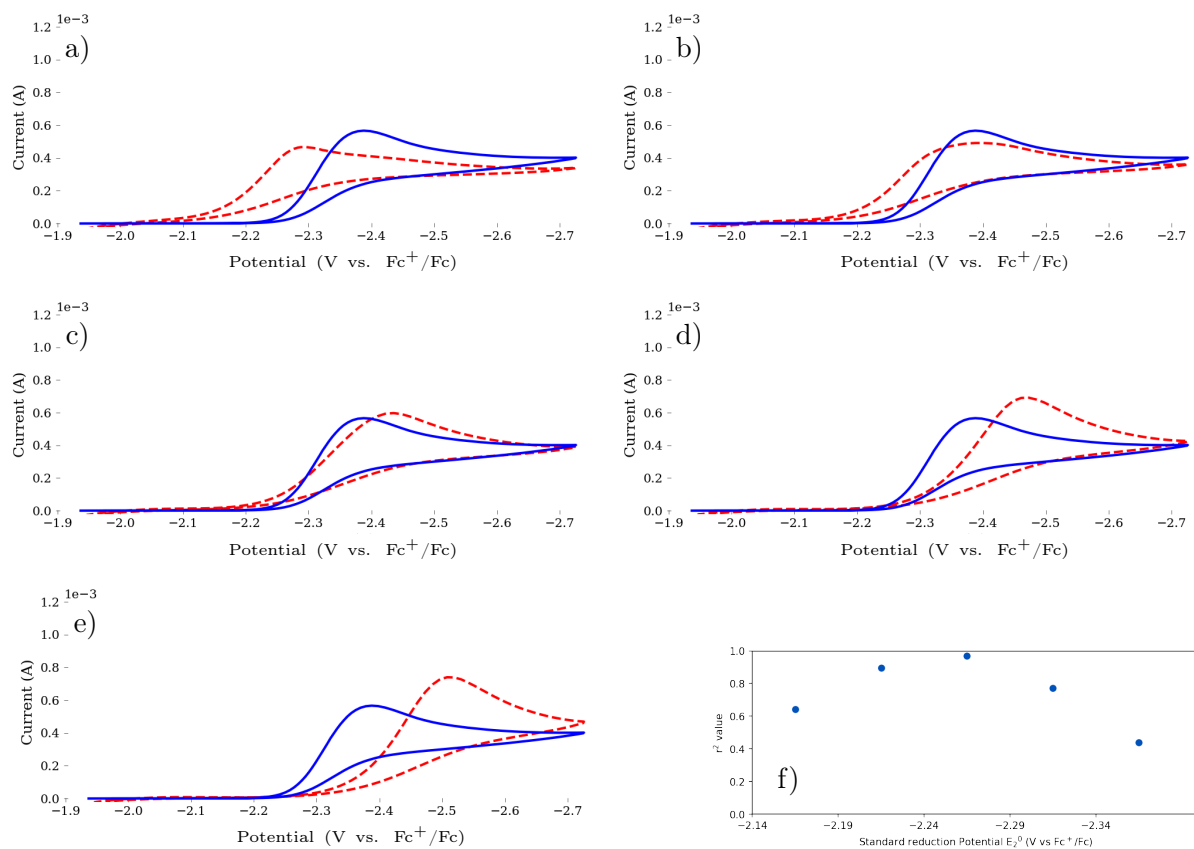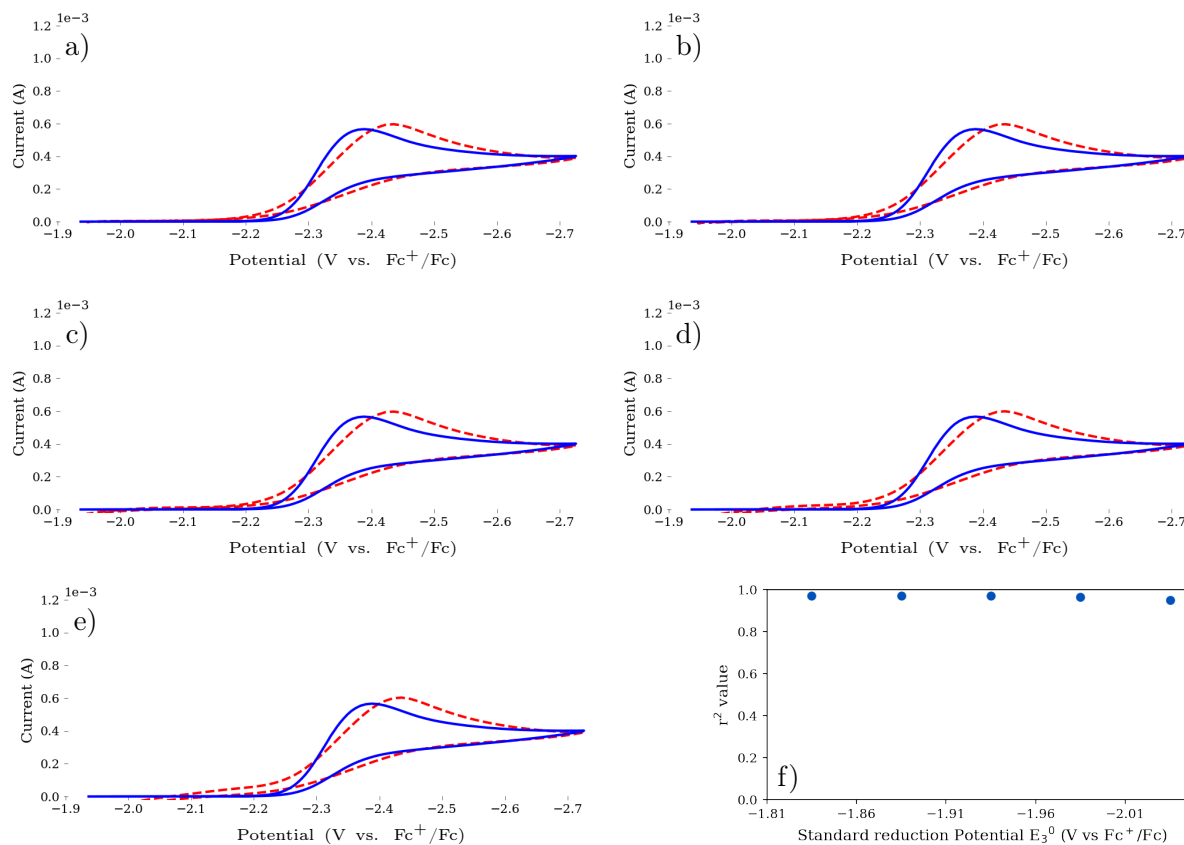
Figure S7. Sensitivity of the COMSOL simulations (dashed) to changes in the value of E_1^0 vs experimental cyclic voltammetry data (solid) for values (a) -2.17, (b) -2.22, (c) -2.27, (d) -2.32, and (e) -2.37 (V vs. Fc^+/Fc) at 13.8 bar CO_2 pressure and 200 mVs^{-1}. The r^2 values at various parameter values are shown in panel (f).
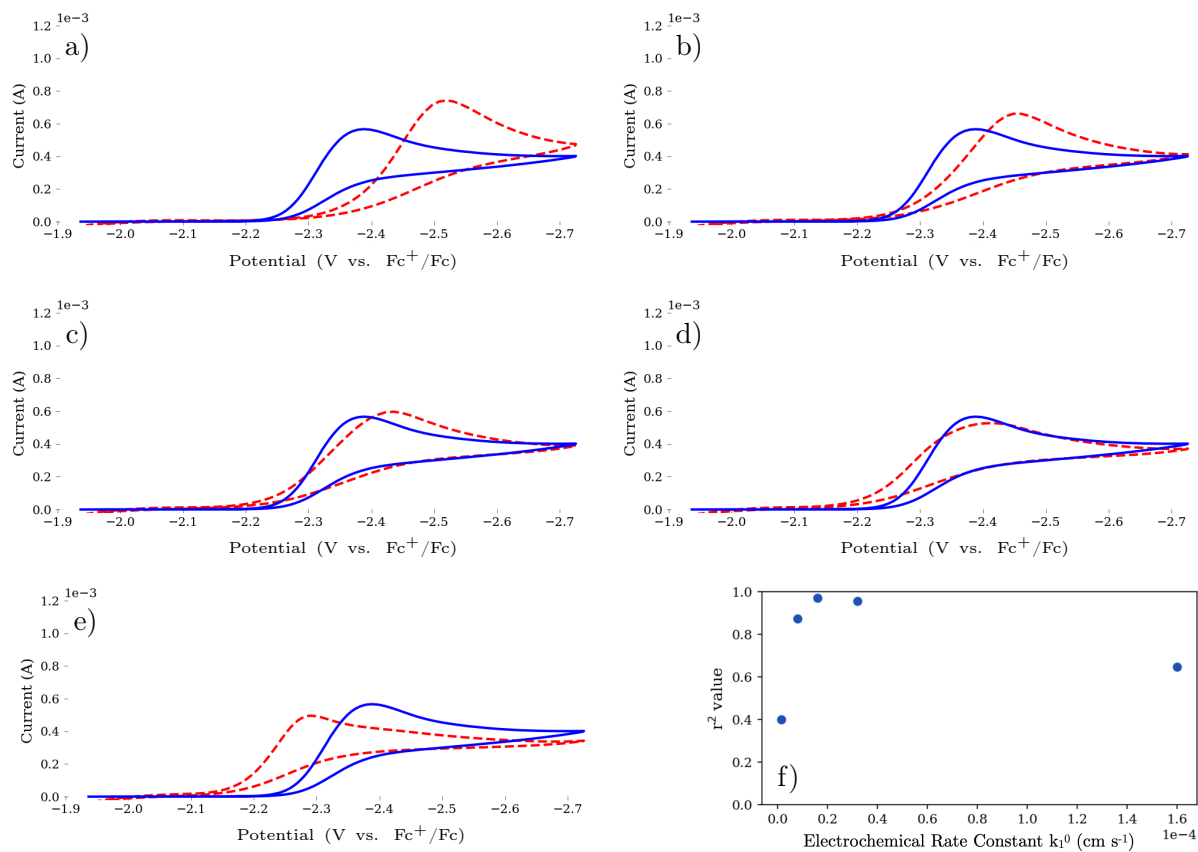
Figure S8. Sensitivity of the COMSOL simulations (dashed) to changes in the value of E_3^0 vs experimental cyclic voltammetry data (solid) for values (a) -1.84, (b) -1.89, (c) -1.94, (d) -1.99, and (e) -2.04 (V vs. Fc^+/Fc) at 13.8 bar CO_2 pressure and 200 mVs^{-1}. The r^2 values at various parameter values are shown in panel (f).
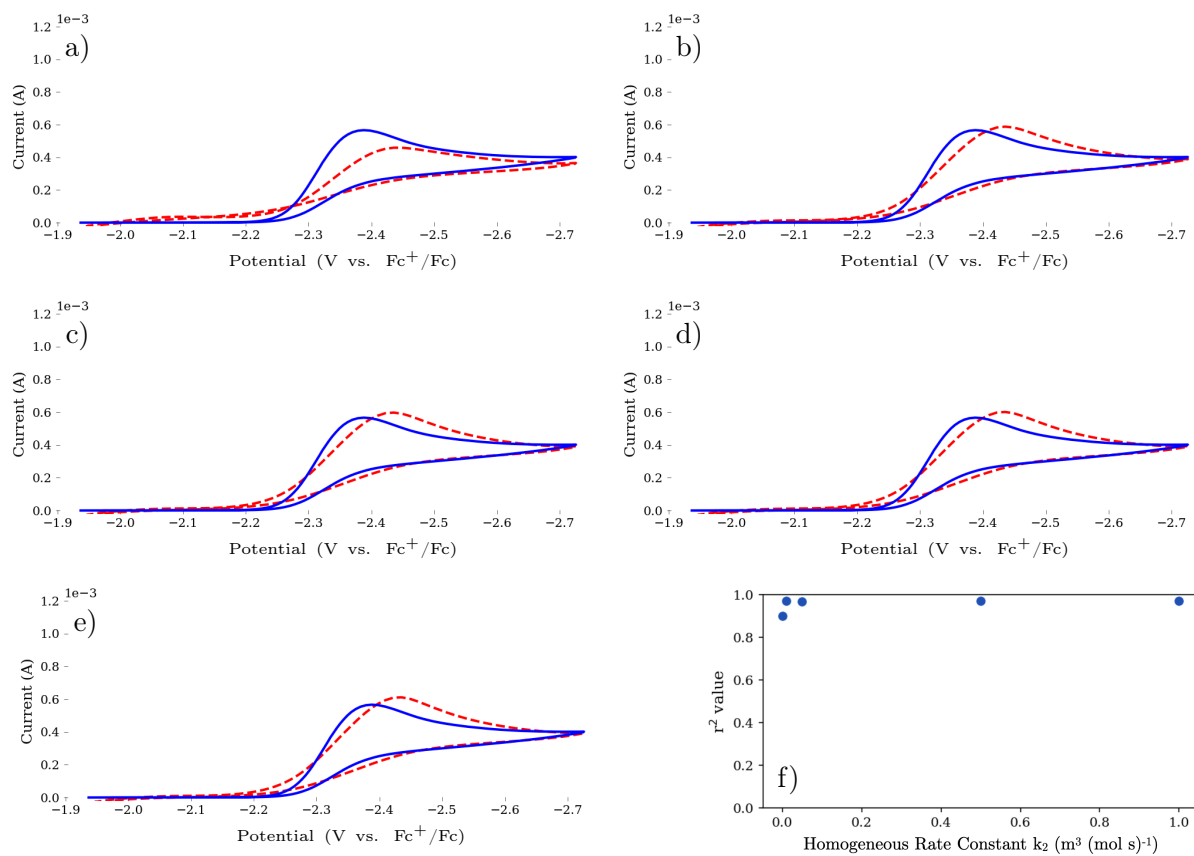
Figure S9. Sensitivity of the COMSOL simulations (dashed) to changes in the value of k_1^0 vs experimental cyclic voltammetry data (solid) for values (a) 1.6e-6, (b) 8e-6, (c) 1.6e-5, (d) 3.2e-5, and (e) 1.6e-4 (cm/s) at 13.8 bar CO_2 pressure and 200 mVs^{-1}. The r^2 values at various parameter values are shown in panel (f).

Figure S10. Sensitivity of the COMSOL simulations (dashed) to changes in the value of k_2 vs experimental cyclic voltammetry data (solid) for values (a) 1e-3, (b) 5e-2, (c) 1e-1, (d) 2e-1, and (e) 1 ($m^3/(s\ mol)$) at 13.8 bar and 200 mVs^{-1}. The r^2 values at various parameter values are shown in panel (f).
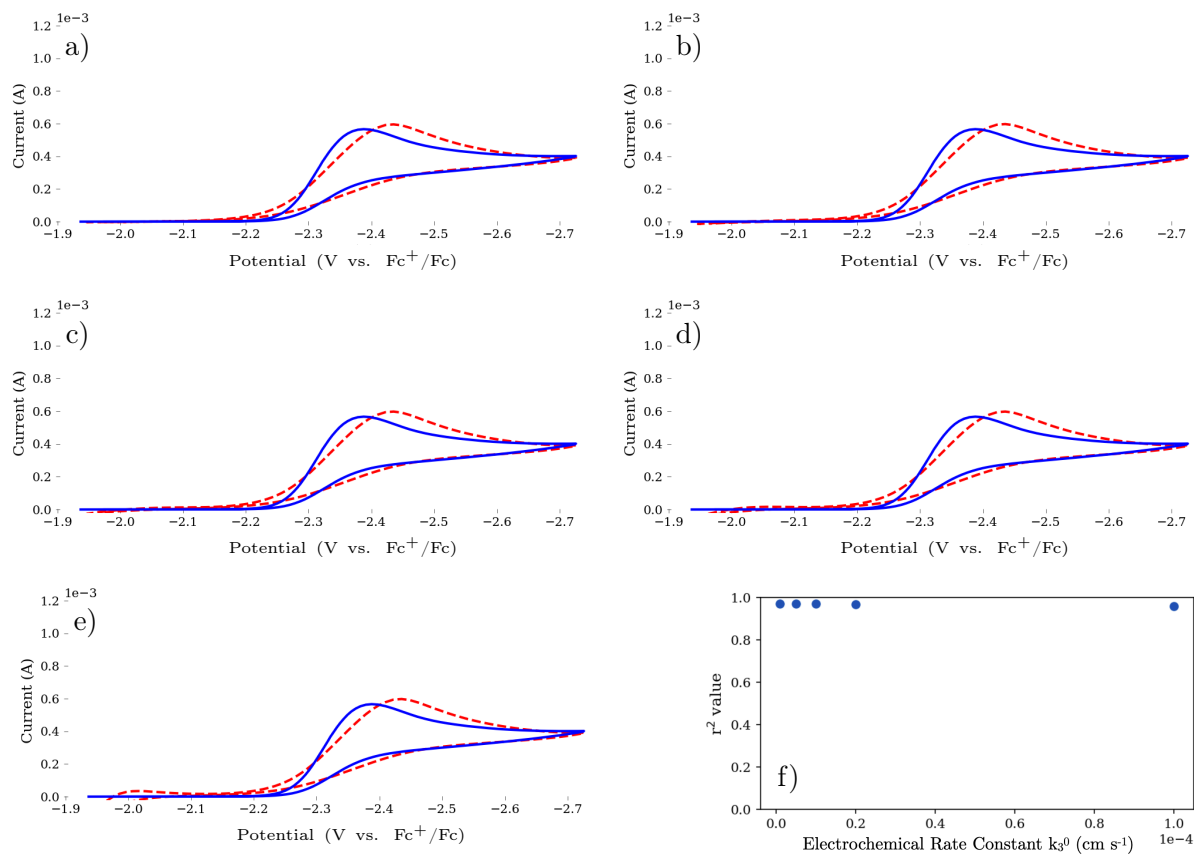
Figure S11. Sensitivity of the COMSOL simulations (dashed) to changes in the value of k_3^0 vs experimental cyclic voltammetry data (solid) for values (a) 1e-6, (b) 5e-6, (c) 1e-5, (d) 2e-5, and (e) 1e-4 (cm/s) at 13.8 bar CO_2 pressure and 200 mVs^{-1}. The r^2 values at various parameter values are shown in panel (f).
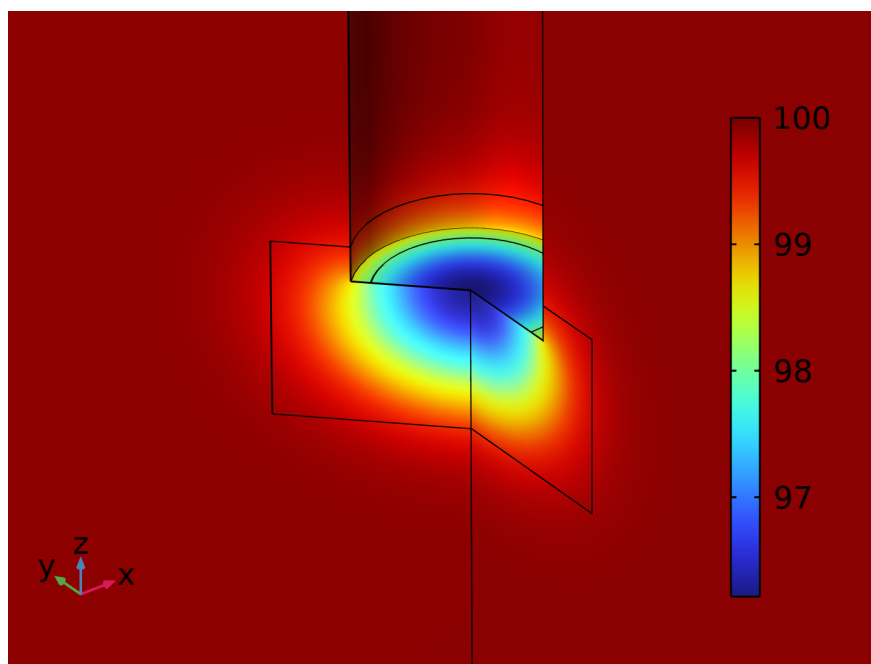
Figure S12. Example COMSOL simulation showing the time-dependent three-dimensional diffusion profile of acetophenone during the cyclic voltammetry experiment. Scale bar shows the concentration of acetophenone in $\mathrm{mol\,m^{-3}}$.

4 References

(1) Shaughnessy, C. I.; Sconyers, D. J.; Kerr, T. A.; Lee, H.-J.; Subramaniam, B.; Leonard, K. C.; Blakemore, J. D. Intensified Electrocatalytic CO_2 Conversion in Pressure-Tunable CO_2-Expanded Electrolytes. *ChemSusChem* **2019**, *12*, 3761–3768.

(2) Stalcup, M. A.; Nilles, C. K.; Lee, H. J.; Subramaniam, B.; Blakemore, J. D.; Leonard, K. C. Organic Electrosynthesis in CO_2-eXpanded Electrolytes: Enabling Selective Acetophenone Carboxylation to Atrolatic Acid. *ACS Sustain. Chem. Eng.* **2021**, *9*, 10431–10436.

(3) Silvestri, G.; Gambino, S.; Filardo, G. Electrochemical carboxylation of aldehydes and ketones with sacrificial aluminum anodes. *Tetrahedron Letters* **1986**, *27*, 3429–3430.